



## Gamma-ray albedo of the moon

I. V. MOSKALENKO<sup>1,2</sup>, T. A. PORTER<sup>3</sup>

<sup>1</sup>*Hansen Experimental Physics Laboratory, Stanford University, Stanford, CA 94305, U.S.A.*

<sup>2</sup>*Kavli Institute for Particle Astrophysics and Cosmology, Stanford University, CA 94309, U.S.A.*

<sup>3</sup>*Santa Cruz Institute for Particle Physics, University of California, Santa Cruz, CA 95064, U.S.A.*

*imos@stanford.edu*

**Abstract:** We use the GEANT4 Monte Carlo framework to calculate the  $\gamma$ -ray albedo of the Moon due to interactions of cosmic ray (CR) nuclei with moon rock. Our calculation of the albedo spectrum agrees with the EGRET data. We show that the spectrum of  $\gamma$ -rays from the Moon is very steep with an effective cutoff around 3 GeV (600 MeV for the inner part of the Moon disc). Since it is the only (almost) black spot in the  $\gamma$ -ray sky, it provides a unique opportunity for calibration of  $\gamma$ -ray telescopes, such as the forthcoming Gamma Ray Large Area Space Telescope (GLAST). The albedo flux depends on the incident CR spectrum which changes over the solar cycle. Therefore, it is possible to monitor the CR spectrum using the albedo  $\gamma$ -ray flux. Simultaneous measurements of CR proton and helium spectra by the Payload for Antimatter Matter Exploration and Light-nuclei Astrophysics (PAMELA), and observations of the albedo  $\gamma$ -rays by the GLAST Large Area Telescope (LAT), can be used to test the model predictions and will enable the GLAST LAT to monitor the CR spectrum near the Earth beyond the lifetime of PAMELA.

## Introduction

Interactions of Galactic CR nuclei with the atmospheres of the Earth and the Sun produce albedo  $\gamma$ -rays due to the decay of secondary neutral pions and kaons (e.g., [10, 7]). Similarly, the Moon emits  $\gamma$ -rays due to CR interactions with its surface [6, 11]; low energy  $\gamma$ -ray spectroscopy data acquired by the Lunar Prospector were used to map the elemental composition of the Moon surface [4, 8]. However, contrary to the CR interaction with the gaseous atmospheres of the Earth and the Sun, the Moon surface is solid, consisting of rock, making its albedo spectrum unique.

Due to the kinematics of the collision, the secondary particle cascade from CR particles hitting the Moon surface at small zenith angles develops deep into the rock making it difficult for  $\gamma$ -rays to get out. A small fraction of all produced pions, splash albedo pions, are mostly low energy ones thus producing the soft spectrum  $\gamma$ -rays. High-energy  $\gamma$ -rays can be produced by CR particles hitting the Moon surface in a close-to tangential direction. However, since it is a solid target, only the

very thin limb contributes to the high energy emission.

The  $\gamma$ -ray albedo of the Moon has been calculated by Morris [6] using a Monte Carlo code for cascade development in the Earth's atmosphere that was modified for the Moon conditions. The Moon has been detected by the EGRET as a point source with integral flux  $F(>100 \text{ MeV}) = (4.7 \pm 0.7) \times 10^{-7} \text{ cm}^{-2} \text{ s}^{-1}$  [11] consistent with the predictions. The observed spectrum is steep and yields only the upper limit  $\sim 5.7 \times 10^{-12} \text{ cm}^{-2} \text{ s}^{-1}$  above 1 GeV.

We report preliminary results for calculations of the  $\gamma$ -ray albedo from the Moon using the GEANT4 [1] framework code and discuss the consequences of its measurement by the upcoming GLAST mission.

## Monte Carlo simulations

In the present work, we use version 8.2.0 of the GEANT4 toolkit. Figure 1 illustrates our beam/target/detector setup for simulating CR inter-

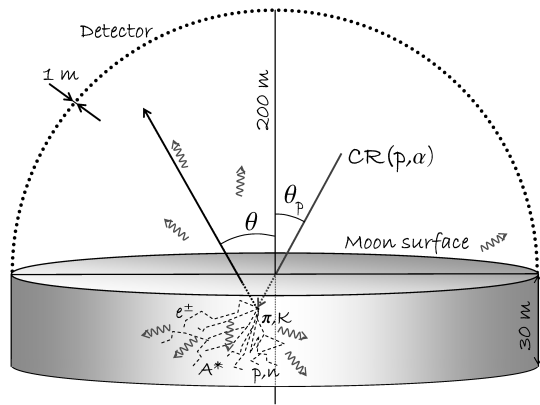


Figure 1: Beam/target/detector setup for simulating CR interactions in moon rock. The primary beam enters the moon rock target with incident polar angle  $\theta_p$ . Secondary  $\gamma$ -rays are emitted with polar angle  $\theta$ . The detection volume surrounds the target.

actions in the Moon. The primary CR beam (protons, helium nuclei) is injected at different incident angles into a moon rock target. We take the composition of the moon rock to be 45%  $\text{SiO}_2$ , 22%  $\text{FeO}$ , 11%  $\text{CaO}$ , 10%  $\text{Al}_2\text{O}_3$ , 9%  $\text{MgO}$ , and 3%  $\text{TiO}_2$  by weight, consistent with mare basalt meteorites and Apollo 12 and 15 basalts [4, 2, 8]. A thin hemispherical detector volume surrounding the target is used to record the secondary  $\gamma$ -ray angular and energy distributions in the simulation.

Let  $d^2Y_\gamma(E_p, \cos\theta_p)/d\log E_\gamma d\Omega$  be the  $\gamma$ -ray yield per logarithmic energy interval and unit solid angle per primary particle with kinetic energy/nucleon  $E_p$  and incident polar angle  $\theta_p$ . The  $\gamma$ -ray yield is calculated using the GEANT4 beam/target setup with a Monte Carlo method.

Figure 2 shows the secondary  $\gamma$ -ray yields integrated over all emission angles outward from the Moon surface for protons with  $E_p = 500$  MeV and 5000 MeV at incident angles  $\cos\theta_p = 0.1$  and 1, respectively. The shapes of the yield curves for different incident angles are very similar to each other for the case of low energy protons where the secondary particles (pions, kaons, neutrons, etc.) are produced nearly at rest. In this case the  $\gamma$ -ray emission is produced in a number of processes: pion

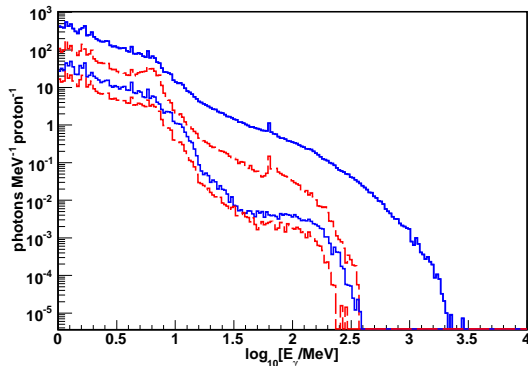


Figure 2:  $\gamma$ -ray yield per proton interaction integrated over all emission angles from the Moon surface. Line-styles: red-dashed,  $\cos\theta_p = 1$ ; blue-solid,  $\cos\theta_p = 0.1$ . Line-sets: lower,  $E_p = 500$  MeV; upper,  $E_p = 5000$  MeV.

and kaon decay, secondary electron and positron bremsstrahlung, and so forth. A considerable flux of  $\gamma$ -rays is produced in nuclear reactions such as neutron capture and nonelastic scattering [4, 8]; the features below  $\sim 10$  MeV are due to nuclear de-excitation lines, where the most prominent contribution comes from oxygen nuclei. In the high energy case, the secondary distribution for protons incident near zenith has a cutoff above  $\sim 500$  MeV. Further away from zenith higher yields of secondary  $\gamma$ -rays are produced while the spectrum of  $\gamma$ -rays become progressively harder. This is a result of the cascade developing mostly in the forward direction: for near zenith primaries, most high energy secondary  $\gamma$ -rays will be absorbed in the target, while a small fraction of produced pions and kaons, splash albedo particles, mostly low energy ones, produce the soft spectrum  $\gamma$ -rays; further from zenith, the high energy secondary  $\gamma$ -rays will shower out of the Moon surface.

## Calculations

The CR spectrum above the geomagnetic cutoff near Earth (at 1 AU) can be directly measured by balloon-borne instruments or spacecraft. However, it has been done during short flights at different phases of solar activity. To calculate the Moon

particle	$J_0$	$a_1$	$b_1$	$c_1$	$a_2$	$b_2$	$c_2$	$a_3$	$b_3$	$c_3$
proton	$1.6 \times 10^4$	1	0.458	2.75	-3.567	0.936	4.90	$4.777 \times 10^5$	14.4	6.88
helium	$1.6 \times 10^3$	1	1.116	3.75	2.611	4.325	3.611	0.219	0.923	2.58

Units of the flux:  $\text{m}^{-2} \text{s}^{-1} \text{sr}^{-1} (\text{GeV/nucleon})^{-1}$ .

Table 1: Fits to local interstellar CR spectra

albedo at an arbitrary modulation level, we use the local interstellar spectra (LIS) of CR protons and helium as fitted to the numerical results of GALPROP propagation model (reacceleration and plain diffusion models, Table 1 in [9]); the CR particle flux at an arbitrary phase of solar activity at 1 AU can then be estimated using the force-field approximation [3].

To fit the LIS CR spectra we choose a function of the form:

$$\frac{dJ_p}{dE_k} = J_0 \sum_{i=1}^3 a_i (E_k + b_i)^{-c_i}, \quad (1)$$

where the flux units are  $\text{m}^{-2} \text{s}^{-1} \text{sr}^{-1} (\text{GeV/nucleon})^{-1}$  and the parameter values are given in Table 1. The latter are not unique and other sets could produce similar quality fits, but this does not affect the final results.

Figure 3 shows the calculated total  $\gamma$ -ray albedo spectrum for CR protons and helium compared to the EGRET data for periods of lower solar (upper solid:  $\Phi = 500$  MV) and higher solar activity (lower solid:  $\Phi = 1500$  MV). Taking into account that the exact CR spectra during the EGRET observations are unknown, the agreement with the data is remarkable. The broken lines show the spectra from the limb (outer 5') and the central part of the disc (20' across) for the case of higher solar activity. As expected, the spectra from the limb and the central part are similar at lower energies ( $<10$  MeV); at high energies the central part exhibits a softer spectrum so that virtually all photons above  $\sim 600$  MeV are emitted by the limb.

Interestingly, the pion annihilation line is still significant even when the  $\gamma$ -ray yields are integrated over the spectrum of CR, although, its intensity is small relative to the total albedo flux. The line perhaps always exists due to the splash albedo particles, but in case of a thin and/or gaseous target (usual in astrophysics) it is indistinguishable from the background  $\gamma$ -rays. For the case of a thick solid

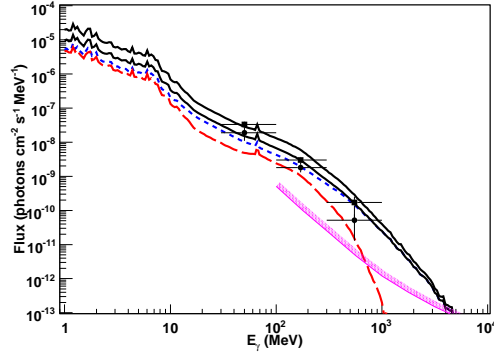


Figure 3: Calculated  $\gamma$ -ray albedo spectrum of the Moon. Line-styles: black-solid, total; blue-dotted, limb – outer 5'; red-dashed, centre – inner 20'. Upper solid line:  $\Phi_0 = 500$  MV; lower solid line:  $\Phi_0 = 1500$  MV. Data points from the EGRET [11] with upper and lower symbols corresponding to periods of lower and higher solar activity, respectively. The differential 1 year sensitivity of the LAT is shown as the hatched region.

rock target, and thus fast energy dissipation of the particle cascade, and because of the kinematics of the interaction, the continuum  $\gamma$ -ray background is much smaller revealing the narrow line from pion annihilation at rest.

## Discussion and Conclusions

The Large Area Telescope (LAT) high-energy  $\gamma$ -ray telescope is scheduled for launch by NASA in winter of 2008. It will have superior angular resolution and effective area, and its field of view (FOV) will far exceed that of its predecessor EGRET [5]. The LAT will scan the sky continuously providing complete sky coverage every two orbits (approximately 3 hr). About 20% of the time

the Moon will be in the FOV at different viewing angles. The point spread function (PSF) of the instrument is about twice the angular diameter of the Moon,  $1^\circ$ , at 1 GeV, but reduces dramatically at higher energies:  $\sim 0.3^\circ$  at 2 GeV and  $\sim 0.1^\circ$  at 10 GeV.

The Moon with its steep albedo spectrum presents almost a black spot on the  $\gamma$ -ray sky above  $\sim 2$  GeV. The central part of the Moon has an even steeper spectrum with a cutoff at  $\sim 600$  MeV. The albedo spectrum of the Moon is well understood while the Moon itself is a “moving target” passing through high Galactic latitudes and the Galactic centre region. This makes it a useful “standard candle” for the GLAST LAT at energies below 1 GeV. A simultaneous presence of the PAMELA on-orbit capable of measuring protons and light nuclei with high precision provides a necessary input for accurate prediction of the albedo flux and a possible independent calibration of the GLAST LAT. An additional bonus of such a calibration is the possibility to use GLAST observations of the Moon to monitor the CR spectra near the Earth beyond the projected lifetime of the PAMELA (currently 3 years).

The line feature around 67.5 MeV from  $\pi^0$ -decay produced by CR particles in the solid rock target is interesting. The lower energy limit of the LAT instrument is below 20 MeV while the energy resolution is  $\sim 15\%$  at 100 MeV, and improves at higher energies. With a suitable event selection it may be possible to observe the line. There is no other astrophysical object predicted to produce such a narrow line and there is no other line expected except, perhaps, from dark matter annihilation. A possibility for energy calibration at higher energy is provided by the steep cutoff of the albedo spectrum above a few GeV. We are investigating the feasibility of these ideas with the GLAST simulation software.

The  $\gamma$ -ray albedo of the Moon makes it a unique calibration target for  $\gamma$ -ray telescopes. The albedo of the Moon is dim, especially its central part at high energies. Its lower energy part exhibits a narrow pion annihilation line, perhaps unique in astrophysics and never before observed, while its continuum intensity depends on the phase of the solar cycle and allows one to monitor the ambient spec-

trum of CR particles. GLAST LAT instrument is well suited for such observations.

## Acknowledgements

We thank Bill Atwood, Seth Digel, Robert Johnson, and Denis Wright for many useful discussions. I. V. M. acknowledges partial support from NASA Astronomy and Physics Research and Analysis Program (APRA) grant. T. A. P. acknowledges partial support from the US Department of Energy.

## References

- [1] Agostinelli, S., et al., *Nuc. Instr. Meth. Phys. Res. A* **506**, 250 (2003).
- [2] Anand, M., et al., *Meteoritics & Planetary Science* **38**, 485 (2003).
- [3] Gleeson, L. J. & Axford, W. I., *ApJ* **154**, 1011 (1968).
- [4] Lawrence, D. J., et al., *Science* **281**, 1484 (1998).
- [5] McEnery, J. E., Moskalenko, I. V., & Ormes, J. F., in *Cosmic Gamma-Ray Sources*, eds. Cheng, K. S. & Romero, G. E., (Dordrecht: Kluwer), *Astrophys. & Spa. Sci. Library* **304**, 361, (2004).
- [6] Morris, D. J., *J. Geophys. Res. A* **89**, 10685 (1984).
- [7] Orlando, E., Petry, D., & Strong, A. W., to appear in *Proc. 1<sup>st</sup> Int. GLAST Symp.* (Stanford, Feb. 5-8, 2007), eds. Ritz, S., Michelson, P. F., & Meegan, C., *AIP Conf. Proc.*, astro-ph/0704.0462.
- [8] Prettyman, T. H., et al., *J. Geo. Phys. Res.* **111**, 12007 (2006).
- [9] Ptuskin, V. S., Moskalenko, I. V., Jones, F. C., Strong, A. W., & Zirakashvili, V. N., *ApJ* **642**, 902 (2006).
- [10] Seckel, D., Stanev, T., & Gaisser, T. K., *ApJ* **382**, 652 (1991).
- [11] Thompson, D. J., Bertsch, D. L., Morris, D. J., & Mukherjee, R., *J. Geophys. Res. A* **120**, 14735 (1997).